Switching Characteristics and Efficiency Improvement with Auxiliary Resonant Snubber Based Soft-Switching Inverters

C.C. Chan, K.T. Chau, D.T.W. Chan
Department of Electrical & Electronic Engineering
The University of Hong Kong
Pokfulum Road, Hong Kong

Jianming Yao
Department of Electrical & Computer Engineering
University of Wisconsin-Madison
Madison, WI 53706-1691,USA

Jih-Sheng Lai, Yong Li
Virginia Power Electronics Center
Virginia Polytechnic Institute and State University
Blacksburg, VA 24061-0111,USA

ABSTRACT - The auxiliary resonant snubber inverter (RSI) has demonstrated superiority in reduction of switching losses and d*v*/d*t*. It was found that the overall inverter system efficiency might not be improved if the resonant current was not controlled in accordance with the load current. This paper proposes an improved control scheme to minimize the operation of auxiliary circuit for efficiency improvement. The principle of this control scheme is to vary the resonant current with variable timing control based on the load current magnitude and to disable the auxiliary circuit operation when diode freewheeling occurs after switching. To illustrate the operation of this control scheme, this paper compares the switching characteristics and inverter power loss of hard-switching inverter, RSI with fixed-timing and variable-timing control and RSI with the proposed control scheme. Experimental results fully agree with the analyses and prove that the proposed control scheme is suitable for RSI to achieve better operating conditions.

I. INTRODUCTION

Recently several auxiliary resonant snubber based inverter (RSI) circuits were proposed to achieve soft switching for high efficiency power conversions [1~10]. The basic concept of RSI is to utilize the resonant snubber capacitor across the device to achieve nearly zero turn-off loss with a lower d*v*/d*t* and to create resonance among the auxiliary inductors and resonant capacitors with an auxiliary switch to achieve zero-voltage turn-on. The auxiliary switch does not turn on until the main switches require a transition from one state to another state. When the auxiliary switch turns on, a resonant pulse diverts the current from upper or lower switch to its opposite-side diode in the same phase leg. After the anti-paralleled diode is conducting, the main switch can be turned on at zero-voltage switching (ZVS). The auxiliary switch is then turned off with zero-current switching (ZCS) when the current in the auxiliary circuit swings down to zero. In the circuit layout, the parasitic inductance and the stray capacitance can be absorbed as a part of resonant components without creating over-voltage or over-current penalty in the inverter's main switches. Thus, these soft-switching inverters potentially achieve high-efficiency power conversion in a cost-effective way.

Figs. 1 and 2 represent two typical RSIs, i.e., Y- and Δ-configured RSIs. Although the device contains certain output capacitance, the resonant capacitors are normally externally added to reduce d*v*/d*t* and turn-off losses because the device output capacitance is too small to achieving snubbing effect. Among all the RSIs, the latest published one, Δ-configured RSI is more attractive one because its advantages of high power capability, no floating-voltage or over-voltage penalty on the auxiliary switches, and no need of using additional voltage or current sensors to achieve soft-switching operation.

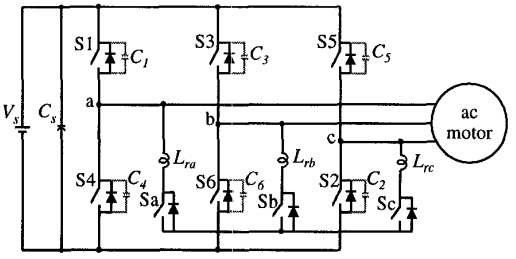

Fig. 1. A Y-configured RSI circuit.

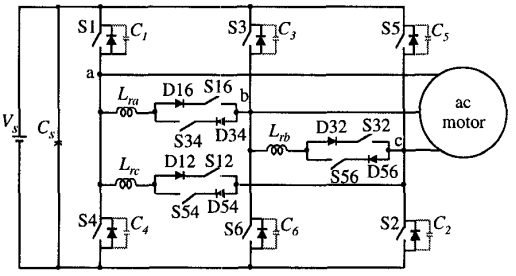

Fig. 2. A Δ-configured RSI circuit.

However, soft-switching inverters reduce the switching power losses in the main circuit while introducing additional power losses in the auxiliary circuit. It is found that the efficiency of the overall inverter system may not be improved or even worse if the switching frequency is high and the resonant current pulse was not controlled in accordance with the load current magnitude and direction. The case could be more noticeable in low-voltage IGBT based inverters where the conduction loss is a dominant loss factor. Therefore, it is the purpose of this paper to introduce an

0-7803-4489-8/98/$10.00 © 1998 IEEE

improved control scheme for RSIs to minimize the operation time of the auxiliary circuit while maintaining ZVS on the main switches.

This paper compares switching characteristics for the cases of hard-switching without any snubber, hard-switching with snubber capacitors and soft-switching with resonant snubbers. With the basis of switching characteristics, the paper then explains how to improve the efficiency with the proposed control. Complete theoretical analyses, computer simulations, hardware implementation, and experimental results will be provided. Finally, it concludes that the RSI topology can obtain better efficiency with the proposed control scheme.

II. Switching Characteristics

To measure switching waveforms for both turn-on and turn-off, three types of inverter cells were constructed, as shown in Fig. 3. Fig. 3(a) is a traditional full-bridge hard-switching inverter cell without any snubber circuits. Fig. 3(b) is the capacitor-snubbed hard-switching inverter cell that allows soft turn-off but worsens turn-on condition. Fig. 3(c) is a full-bridge RSI cell.

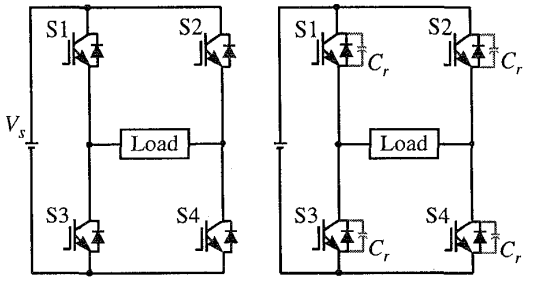

(a) A full-bridge hard-switching cell

(b) A full-bridge capacitor snubbed hard-switching cell

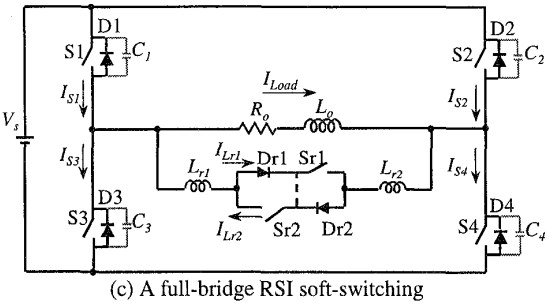

(c) A full-bridge RSI soft-switching

Fig. 3. Different switching configurations for a full-bridge inverter cell.

The hardware experiments were implemented step by step. Firstly, a single-phase traditional hard-switching inverter was built. Secondly, with the snubber capacitors added, it turned into the hard-switching inverter with snubber capacitors. Finally, the soft-switching inverter was constructed by adding the auxiliary circuit.

The components and their values are summarized as follows:

Main circuit:

- Main switches: TOSHIBA IGBT MG100H2YS1
- Snubber capacitors: 47nF
- Inductive load: 2.5mH

Auxiliary circuit:

- Auxiliary switches: IR IGBT IRGBC30KD2
- Resonant Inductors: 5μH

A. Hard-Switching Inverter without Snubbers

It was found that the natural freewheeling of the anti-paralleled diode could achieve soft switching for the main switches. This soft-switching phenomenon can be explained in Fig. 4 (a). For turn-on, it is clear that the gate signal comes after the device voltage drops to zero, meaning that the device turns on when its anti-paralleled diode is conducting. For turn-off, the waveform can be clean if the device current is diverted to the opposite side of the freewheeling diode after the device is gated off.

The widely recognized hard-switching condition can be explained in Fig. 4(b). During turn-on, the device is to shut off the opposite-side diode current, and thus carrying both the load and the diode reverse recovery currents. During turn-off the device does not carry the current, but the anti-paralleled diode does, and the current needs to be shut off until the opposite side device is turned on. Thus, an abrupt current spike occurs that creates circuit noises which can be seen from the gate signals. This type of switching that involves diode reverse recovery current always draws significant switching noises and power losses.

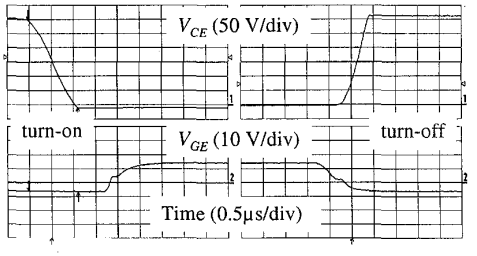

(a) Switch turn-off with opposite-side diode taking over the load current and opposite-side switch turning on at ZVS.

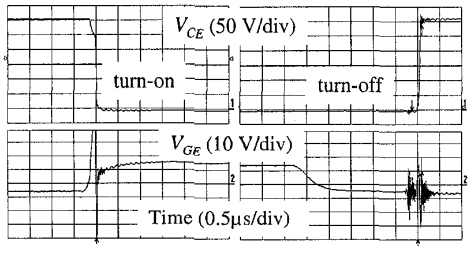

(b) Switch turn-on while opposite-side diode being turn-off

Fig. 4. Hard-switching cell turn-on and turn-off waveforms showing device and gate voltages.

Typical device turn-on current and voltage can be seen in Fig. 5(a). The device current is nearly doubled with respect to the load current due to the addition of the diode reverse recovery current. Device turn-off current and voltage can be seen in Fig. 5(b). There is a turn-off over-voltage that is due to the parasitic inductance and sharp di/dt effect. The switching energies for both turn-on and turn-off were obtained by integrating the product of the device voltage and current over the switching period.

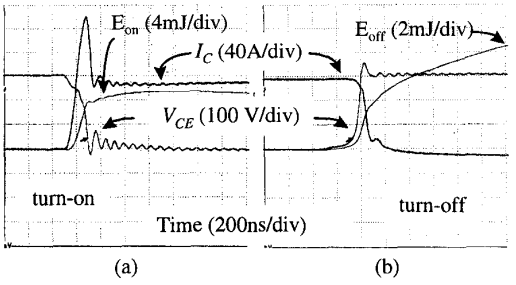

Fig. 5. Hard-switching voltage, current, and energy waveforms. (a) turn-on. (b) turn-off.

B. Hard-Switching Inverter with Snubber Capacitors

Fig. 6 shows the measured waveforms for the hard-switching inverter cell with snubber capacitors as shown in Fig. 3(b). The added capacitors significantly reduce voltage rise-rate during turn-off. However, the device voltage shows a high frequency ringing after switching, which can be attributed to the resonance of the added capacitor and the stray leakage inductance.

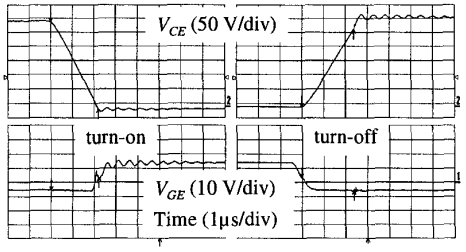

(a) Switch turn-off with opposite-side diode taking over the load current and opposite-side switch turning on at ZVS.

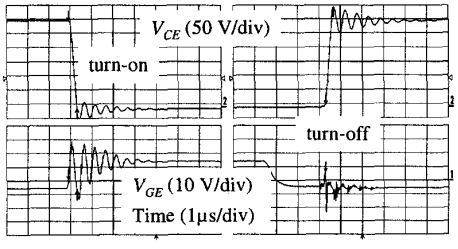

(b) Switch turn-on while opposite-side diode being turn-off

Fig. 6. Capacitor snubbed hard-switching cell turn-on and -off waveforms showing device and gate voltages.

Similar to the condition shown in Fig. 4(b), Fig. 6(b) indicates that the capacitor snubbed circuit cannot avoid switching problem when the device turns on into opposite-side diode being turned off. The energy stored in the capacitors needs to be discharged during turn-on, and thus creating a large current spike within the device.

Fig. 7 shows that during device turn-off, there is a linear capacitor charging period that is similar to the condition in Fig. 6(a). After this linear region and before the device is fully turned off, there is a sharp edge showing that the device is being turned off by the opposite-side switch. The two different dv/dt values are caused by the turn-on of the opposite-side switch before the capacitor is fully charged. This phenomenon typically occurs at light current conditions.

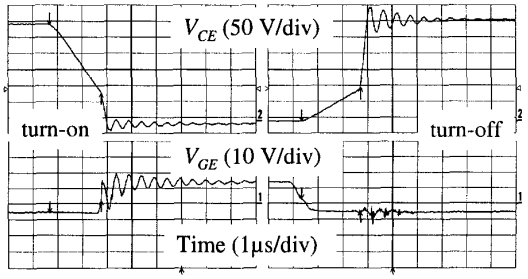

Fig. 7. The capacitor snubbed hard-switching cell turns off slowly to charge the capacitor, but the opposite-side switch turns on before the capacitor is fully charged, resulting two dv/dt values.

C. *Soft-Switching RSI*

The soft-switching condition differs from the above capacitor snubbed hard-switching by adding auxiliary switching to divert the diode reverse recovery current during turn-on. Fig. 8 shows the measured waveforms for the soft-switching RSI cell. The turn-on waveform indicates that the gate voltage turns on after the device voltage drops to zero, and the anti-paralleled diode conducts. Thus, ZVS turn-on is achieved.

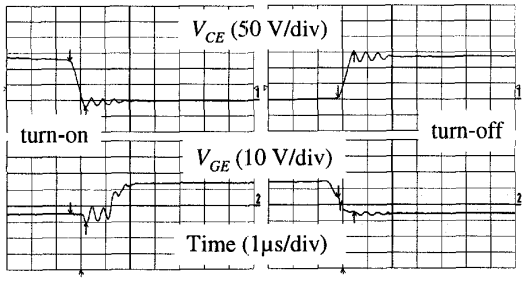

Fig. 8. Soft-switching RSI cell turn-on and turn-off waveforms showing device and gate voltages.

The above step-by-step derivation to achieve soft-switching indicates that the switching characteristics is improved by adding capacitors to help turn-off, and by

adding auxiliary switching to help turn-on. Understanding of such hard- and the soft- switching phenomena is very useful for design improvement of the overall performance of the RSI.

III. Control Schemes

A. Fixed-Timing Control

During the implementation, it was found that the inverter efficiency would be worse than the hard-switching inverter if the resonant circuit timing control were fixed as realized in basic RSI. This is a result contrary to the finding in [4] because unlike using MOSFET as the main device in [4], the device used here is IGBT that has reasonable diode reverse recovery characteristic, and switching loss reduction by fixed timing control is not significant. The principle idea of fixed-timing control is to charge the resonant inductors with a fixed period before every switching state change. This control scheme is very simple and easy to realize.

B. Variable-Timing Control

If the resonant current is not controlled according to the magnitude of the load current, the auxiliary switch will conduct unnecessary time and draw extra current. Under fixed-timing control, the energy charged to the resonant inductor is always the same during every operation of the auxiliary circuit. If this energy is enough for charging and discharging the snubber capacitors when the load current is at its peak value, it would be more than enough at low load condition. By varying the timing control with load current, the efficiency can then be improved because the auxiliary circuit conduction time is reduced.

Fig. 9 shows the load and resonant currents under fixed timing and variable timing control conditions. Fig. 10 indicates the waveform and timing of the resonant current that varies from 4 μs to 7 μs. Efficiency improvement with the variable timing control will be shown later.

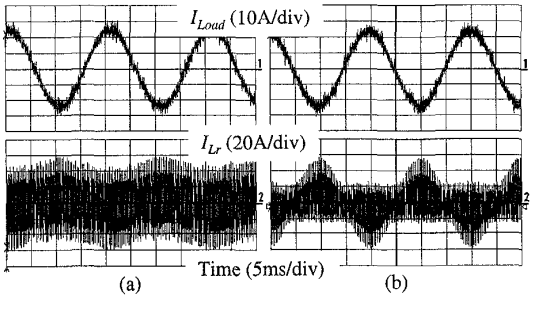

Fig. 9. Soft-switching RSI cell load and resonant inductor current waveforms. (a) fixed timing. (b) variable timing.

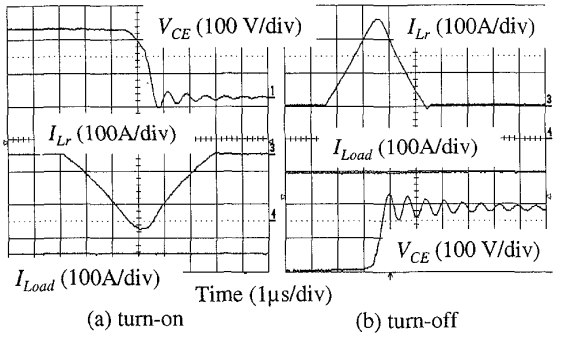

Fig. 10. Soft-switching cell turn-on and turn-off waveforms showing device and gate voltages.

C. An Improved Control Scheme

From the switching characteristics of hard-switching inverter, it was found that the soft switching occurred naturally when the device did not have to turn off the opposite-side diode. Thus, the ZVS can be achieved without the operation of auxiliary circuit when the natural freewheeling can be utilized. The improved control scheme is to fully utilize the natural soft switching and to operate the auxiliary circuit with variable timing control to achieve highest efficiency.

Using Fig. 2 (c) as the example, the operation modes for one complete PWM cycle without using the improved control scheme are illustrated in Fig. 11, while the corresponding theoretical waveforms are shown in Fig. 12(a).

Mode 0 ($t < t_0$) is the initial stage. It is desired to turn off S_1 and S_4, and then to turn on S_2 and S_3.

At t_0 of *Mode 1* ($t_0 \sim t_1$), S_{r1} is turned on, and the resonant inductor current begins to increase linearly which is governed by:

$$V_s = (L_{r1} + L_{r2})\frac{dI_{Lr1}}{dt} = 2L_r \frac{dI_{Lr1}}{dt} \quad (1)$$

where $L_{r1} = L_{r2} = L_r$. Thus, the resonant inductor current and hence the main switch current in both S_1 and S_4 are given by:

$$I_{Lr1} = \frac{V_S}{2L_r}(t - t_0) \quad (2)$$

$$I_{S1} = I_{S4} = I_{Load} + I_{Lr1} = I_{Load} + \frac{V_S}{2L_r}(t - t_0) \quad (3)$$

Since the current in both S_1 and S_4 is the sum of the resonant inductor current and load current, both switches need to draw additional current and consume additional conduction loss in this case.

At t_1 of *Mode 2* ($t_1 \sim t_2$), the turn-off of S_1 and S_4 starts the resonance between the resonant inductors and snubber capacitors. At t_2, C_1 and C_4 are charged to full DC-link voltage while C_2 and C_3 are discharged to zero, thus providing the zero voltage condition for both S_2 and S_3.

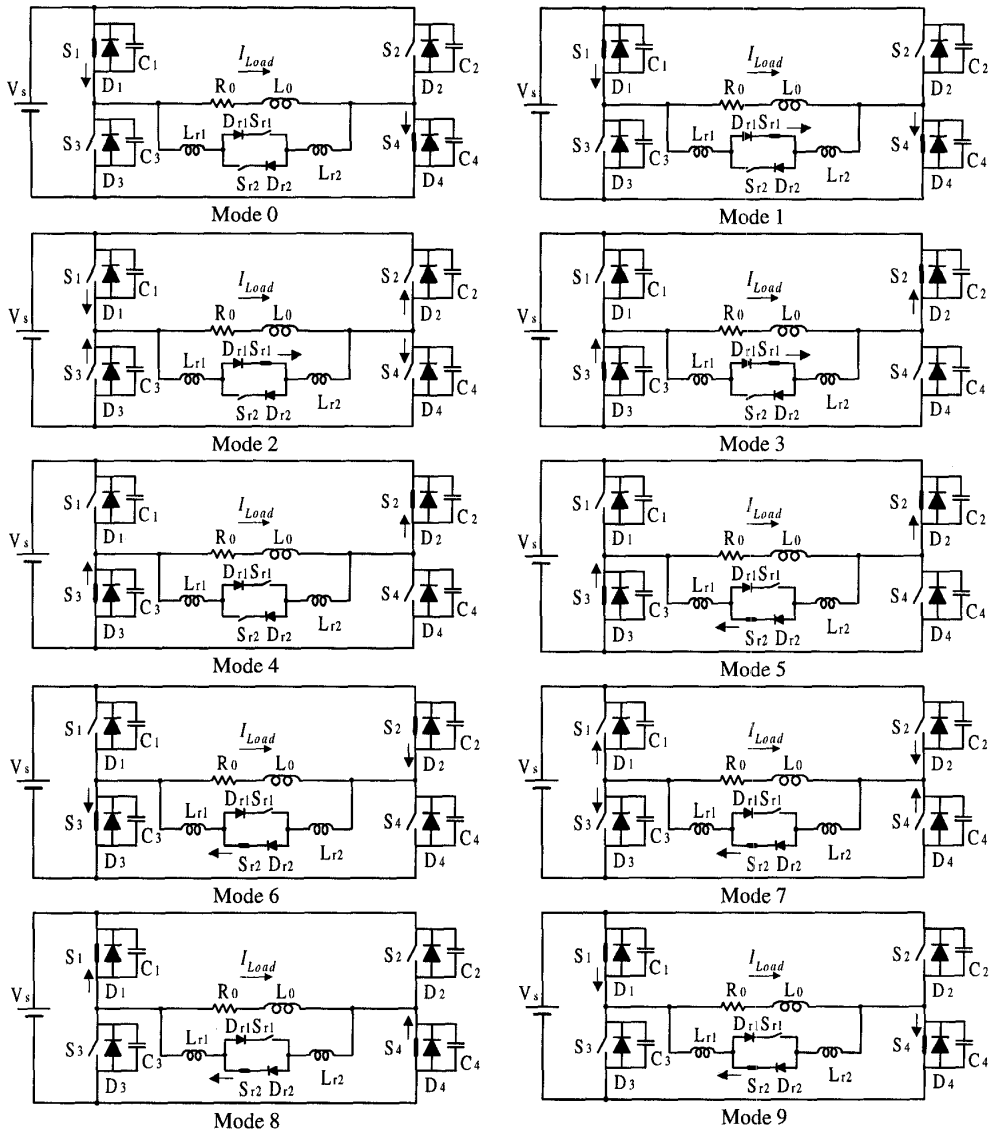

Fig. 11. Modes of operation for basic RSI.

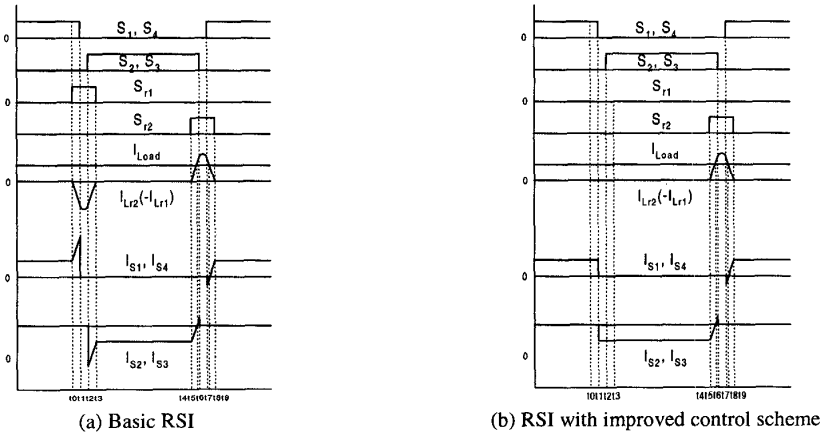

Fig. 12. Theoretical operating waveforms.

At t_2 of *Mode 3* (t_2 ~ t_3), S_2 and S_3 are turned on with ZVS. The resonant inductor current begins to decrease linearly, and both D_2 and D_3 start freewheeling.

At t_3 of *Mode 4* (t_3 ~ t_4), the resonant inductor current is zero so that S_{r1} can be turned off with ZCS. The load current continues freewheeling via D_2 and D_3.

At t_4 of *Mode 5* (t_4 ~ t_5), S_{r2} is turned on. The resonant inductor current begins to increase linearly:

$$V_s = (L_{r1} + L_{r2})\frac{dI_{Lr2}}{dt} = 2L_r \frac{dI_{Lr2}}{dt} \quad (4)$$

$$I_{Lr2} = \frac{V_S}{2L_r}(t - t_4) \quad (5)$$

where $I_{Lr2} = -I_{Lr1}$. Hence, the current in both S_2 and S_3 is given by:

$$I_{S2} = I_{S3} = I_{Load} - I_{Lr1} = I_{Load} - \frac{V_S}{2L_r}(t - t_4) \quad (6)$$

which becomes zero at t_5. The corresponding current in both S_2 and S_3 is always lower than the load current, which is different to that in *Mode 1*.

At t_5 of *Mode 6* (t_5 ~ t_6), the current in both S_2 and S_3 changes the direction. Thus, the resonant inductor current continues to increase, and exceeds the load current. When this inductor current becomes sufficiently high that the stored energy in the resonant inductors can charge and discharge the snubber capacitors, both S_2 and S_3 are turned off at t_6. Therefore, the necessary condition for attaining soft-switching is given by:

$$(L_{r1} + L_{r2})(I_{Lr2} - I_{Load})^2 \geq (C_1 + C_2 + C_3 + C_4)V_S^2 \quad (7)$$

It should be noted that if the resonant inductors are overcharged, an unnecessary over-current and additional conduction loss will be resulted. On the other hand, if they are undercharged, the desired ZVS operation cannot be realised. Therefore, the soft-switching condition largely depends on the duration of *Mode 6*.

At t_6 of *Mode 7* (t_6 ~ t_7), resonance between the resonant inductors and snubber capacitors begins to take place. At t_7, C_2 and C_3 are charged to full voltage while C_1 and C_4 are discharged to zero, thus providing the desired zero voltage condition for turning on S_1 and S_4.

At t_7 of *Mode 8* (t_7 ~ t_8), the resonant inductor current starts to decrease while D_1 and D_4 become conducting. Thus, S_1 and S_4 can be turned on with ZVS. At t_8, the resonant inductor current equals the load current, and the current in both S_1 and S_4 begins to conduct.

In *Mode 9* (t_8 ~ t_9), the resonant current continues to decrease linearly. At t_9, the resonant inductor current decreases to zero so that S_{r2} can be turned off with ZCS. The next operating stage is *Mode 0*, and the whole operating process repeats cyclically.

The proposed control scheme is to skip *Mode 1* through *Mode 3* to disable the operation of the auxiliary circuit because the natural freewheeling can occur. The typical theoretical waveforms are shown in Fig. 12(b).

With the use of this improved control scheme, the auxiliary circuitry needs to operate only about one half of the original time, leading to significant reduction in the additional loss associated with the auxiliary circuit operation. Also, the over-current problem and the corresponding conduction loss in the main switches in the original *Mode 1* can be eliminated.

IV. RESULTS

In order to illustrate the validity of the proposed control scheme, the steady-state waveforms of a practical Δ-RSI are shown with PSpice simulation results. The circuit parameters of this simulation are selected as V_s = 120 V, $L_{r1} = L_{r2}$ = 5 μH and C_1 = C_2 = C_3 = C_4 = 47 nF. The PSpice simulated waveforms are shown in Fig. 13, which compare the cases of basic RSI and RSI with proposed control scheme. These simulated waveforms closely agree with the theoretical analysis. The measured waveforms of the resonant inductor current and load current for the two cases are shown in Fig. 14. Fig. 14(b) indicates that the auxiliary circuit is completely disabled in one current direction.

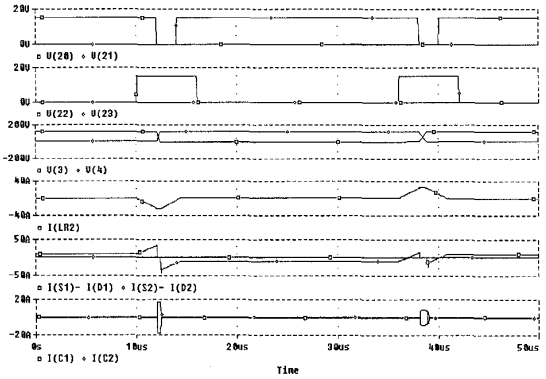

(a) Basic RSI

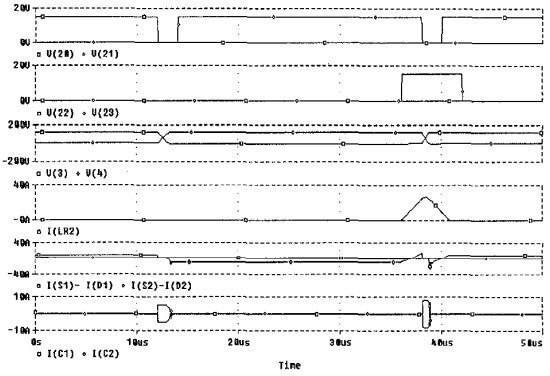

(b) RSI with proposed control.

Fig. 13. PSpice simulation results.

To illustrate the efficiency improvement with the proposed control scheme, the total inverter power losses were measured for the following four cases: 1) hard-switching inverter, 2) RSI with fixed-timing control, 3) RSI with variable-timing control and 4) RSI with proposed control scheme. Fig. 15 clearly indicates that the proposed control scheme is most superior in terms of loss reduction. The major saving is mainly in the reduction of conduction loss in the auxiliary circuitry throughout the operating cycle and the elimination of conduction loss in the main switches during the periods with temporary over-current.

With the basic RSI operation, the temperature rises of the heat sinks for main switches and auxiliary switches were found at 12 °C and 46 °C, respectively. With the proposed control, the corresponding temperature rises were found only 7 °C for both switches, further demonstrating that there is a significant reduction in the inverter power loss.

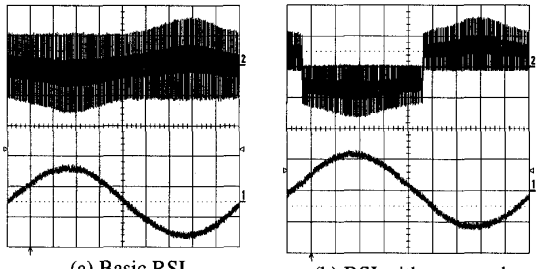

(a) Basic RSI (b) RSI with proposed control.

Fig. 14. Resonant inductor current (upper trace) and load current (lower trace) (20A/div, 2ms/div)

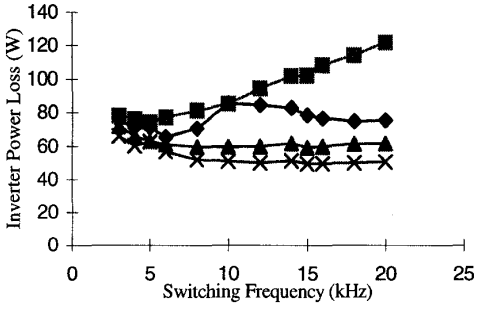

Fig. 15. Power loss comparison for the four cases (from top to bottom): 1) hard-switching inverter, 2) RSI with fixed-timing control, 3) RSI with variable-timing control and 4) RSI with proposed control scheme.

V. Conclusion

In this paper, an improved control scheme for RSI has been presented. The proposed control scheme varies the resonant current according to the load current magnitude and direction. The auxiliary resonant circuit can be disabled when the natural ZVS condition can be utilised. Both theoretical and experimental results illustrate that the total power loss can be significantly reduced. The over-current problem in the main switches can be eliminated by adopting the proposed control. Although the proposed approach has only been exemplified by using a Δ-RSI, it can readily be applied to the whole family of RSIs and extended to other soft-switching inverters.

References

[1] R. W. DeDoncker and J. P. Lyons, "The auxiliary quasi-resonant dc link inverter," in *Conf. Rec. of IEEE PESC*, June 1991, pp. 248–253.

[2] W. McMurray, "Resonant snubbers with auxiliary switches," *IEEE Trans. on Ind. Appl.*, Vol. 29, No. 2, Mar./Apr. 1993, pp. 355–362.

[3] J. S. Lai, R. W. Young, G. W. Ott, J. W. McKeever, and F. Z. Peng, "A delta configured auxiliary resonant snubber inverter," *IEEE Trans. on Ind. Appl.*, Vol. 32, No. 3, May/Jun. 1996, pp. 518–525.

[4] J. S. Lai, R. W. Young, G. W. Ott, C. P. White, J. W. McKeever, and D. S. Chen, "A novel resonant snubber inverter," in *Conf. Rec. of IEEE APEC*, Dallas, TX, Mar. 1995, pp. 797–803.

[5] J. S. Lai, "Resonant snubber-based soft-switching inverters for electric propulsion drives," *IEEE Trans. on Ind. Electr.*, Vol. 44, No. 1, Feb. 1997, pp. 71–80.

[6] S. Frame, D. Katsis, D. H. Lee, D. Borojevic, F. C. Lee, "A three-phase zero-voltage-transition inverter with inductor feedback," in *Proc. of 1996 VPEC Seminar*, Blacksburg, VA, Sep. 1996, pp. 189–193.

[7] V. Vlatovic, D. Borojevic, F. C. Lee, C. Cuadros, and S. Gataric, "A new zero-voltage transition, three-phase PWM rectifier/inverter circuit," in *Conf. Rec. of IEEE PESC*, Seattle, WA, Jun. 1993, pp. 868–873.

[8] W. McMurray, "Resonant snubbers with auxiliary switches," *IEEE Trans. on Ind. Appl.*, Vol. 29, No. 2, Mar./Apr. 1993, pp. 355–362.

[9] C. Cuadros, D. Borojevic, S. Gataric, V. Vlatovic, H. Mao, F. C. Lee, "Space vector modulated, zero-voltage transition three-phase to dc bidirectional converter," *Conf. Rec. of IEEE PESC*, Taipei, Taiwan, June 1994, pp. 16–23.

[10] H. Mao and F. C. Lee, "Improvement on zero-voltage transition three-phase rectifier/inverter," in *Proc. of 1995 VPEC Seminar*, Blacksburg, VA, Sep. 1995, pp. 19–27.